Quasiparticle tunneling spectra of the high-T_c mercury cuprates: Implications of the d-wave two-dimensional van Hove scenario

J. Y. T. Wei*
Department of Applied Physics, Columbia University, New York, New York 10027

C. C. Tsuei
IBM T. J. Watson Research Center, P.O. Box 218, Yorktown Heights, New York 10598

P. J. M. van Bentum
Research Institute for Materials, University of Nijmegen, NL-6525 ED, The Netherlands

Q. Xiong† and C. W. Chu
Texas Center for Superconductivity, University of Houston, Houston, Texas 77204

M. K. Wu
Department of Applied Physics, Columbia University, New York, New York 10027
and Department of Physics and Materials Science Center, National Tsing Hua University, Hsinchu, 30043, Taiwan, Republic of China

(Received 31 January 1997; revised manuscript received 9 June 1997)

Quasiparticle tunneling measurements of the high-temperature superconductors $HgBa_2Ca_{n-1}Cu_nO_{2n+2+\delta}$ (Hg-12$(n-1)n$,n=1,2,3) are considered in the context of $d_{x^2-y^2}$ symmetry of the superconducting order parameter and a two-dimensional (2D) van Hove singularity (vHs) related to saddle points in the electronic band structure. Normal-metal–insulator–superconductor tunneling spectra taken at 4.2 K with a scanning tunneling microscope on Hg-1212 c-axis epitaxial films, as well as on Hg-1201 and Hg-1223 polycrystalline samples, show distinct gap characteristics which cannot be easily reconciled with the simple s-wave BCS density of states. The data are analyzed with the nodal d-wave gap function $\Delta_{\mathbf{k}}=\Delta_0(\cos k_x-\cos k_y)/2$ and the 2D tight-binding electronic dispersion $\xi_{\mathbf{k}}=-2t(\cos k_x+\cos k_y)+4t'(\cos k_x \cos k_y)-\mu$, using the quasiparticle tunneling formalism for elastic and specular transmission. The analysis indicates a highly directional and energy-dependent spectral weighting, related to the gap anisotropy and band-structure dependence of the tunneling matrix element $|T|^2$, and successfully explains the observed gap spectra. Values for the d-wave gap maximum are determined to be $\Delta_0 \approx 33$, 50, and 75 meV, respectively, for optimally doped Hg-1201, Hg-1212, and Hg-1223, corresponding to reduced-gap ratios of $2\Delta_0/k_BT_c \approx 7.9$, 9.5, and 13. These ratios are substantially larger than the BCS weak-coupling limit of 3.54. A comparison with data from other high-T_c cuprates indicates an overall trend of $2\Delta_0/k_BT_c$ rising with T_c, in violation of BCS universality. [S0163-1829(98)05206-0]

I. INTRODUCTION

Tunneling spectroscopy has traditionally been important to the study of superconductivity, providing a sensitive probe of the BCS quasiparticle density of states (DOS) and thus a direct measurement of the superconducting energy gap Δ.[1] For the high-T_c cuprates however, now a decade after their initial discovery,[2,3] quasiparticle tunneling is still not well understood. Experimentally, a remarkable variety of tunneling spectra has been reported,[4–6] generally deviating from ideal BCS behavior and showing large energy gaps ($2\Delta/k_BT_c > 3.54$). Spectral anomalies such as suppressed or enhanced gap singularities, quasilinear conductance background, zero-bias conductance peak, and asymmetry tend to complicate spectral analysis and introduce uncertainty in the gap determination. There is currently no theoretical consensus on this problem. Some workers have considered spectral contributions from extrinsic causes such as chemical inhomogeneity, low barrier heights,[7] and single-electron charging of the junction,[8] in an effort to extract the quasiparticle DOS and to deduce Δ. Others have focused on more intrinsic explanations such as interlayer coupling,[9,10] inelastic scattering by spin-fluctuations, and non-Fermi liquid phenomenology,[11–16] seeking to relate the tunneling anomalies to possible mechanisms responsible for high-T_c superconductivity. Each of the models tends to be specialized to explain one or another of the tunneling anomalies without providing an unifying picture.

A successful theory of quasiparticle tunneling for the high-T_c cuprates should be able to reconcile the disparate spectral behaviors with well-established model assumptions. The d-wave two-dimensional (2D) van Hove scenario provides a very viable model for comparison. First, there is now ample reason to believe that most of the high-T_c cuprates have d-wave pairing symmetry. Recent experiments, particularly the observation of half flux quantum attributed to negative Josephson coupling across π junctions in a tricrystal ring,[17] indicate that the superconducting order parameter

changes sign along the $k_x = \pm k_y$ directions in the ab plane, consistent with the $d_{x^2-y^2}$ pairing symmetry endorsed by most of the current microscopic theories.[18] Second, there is much direct evidence, from high-resolution angle-resolved photoemission (ARPES) measurements[19–21] and corroborating band structure calculations,[22] that most of the high-T_c cuprates have a quasi-2D electronic dispersion with saddle points near the Fermi surface at $\mathbf{X} = (\pm\pi, 0)$ and $\mathbf{Y} = (0, \pm\pi)$ corresponding to a logarithmic van Hove singularity (vHs) in the normal-state DOS. It is natural to consider whether this combination of pairing symmetry and band structure could explain the tunneling characteristics observed, both as a consistency check and to enable proper spectral analysis.

Quasiparticle tunneling in the context of d-wave pairing symmetry has been considered previously,[23–28] but never properly taking into account the characteristic band structure of the cuprates. The standard approach is to calculate the quasiparticle DOS for direct comparison to the tunneling conductance. The matrix element $|T|^2$ for tunneling *into* the cuprate is typically treated as energy independent, isotropic, and nonvanishing only in the ab plane or it is simplified by assuming a narrow tunneling cone which provides high directional selectivity and by invoking the Wentzel-Kramers-Brillouin (WKB) approximation which neglects wave vector matching in the barrier transmission.[29,30] These simplifications are usually made to facilitate model calculations. However, it is not obvious that the tunneling cone argument and the WKB approximation are insensitive to band-structure anisotropy, or valid in the presence of saddle points. Nor is there reason *a priori* to neglect the probability for tunneling perpendicularly *into* the ab plane simply because of the low c-axis dispersion. It is important to consider $|T|^2$ explicitly, in order to relate the calculated quasiparticle DOS to the conductance spectra observed.

The mercury-based cuprates $HgBa_2Ca_{n-1}Cu_nO_{2n+2+\delta}$ [Hg-12$(n-1)n$] offer an attractive system to study this problem.[31–33] Consisting essentially of conducting $(CuO_2)_n$ stacks separated by insulating BaO-Hg-BaO perovskite blocks, the Hg cuprates are an exemplary quasi-2D system with tetragonal symmetry, very low lattice distortion, and exhibiting very high T_c. Band-structure calculations have indicated a characteristic cross-shaped Fermi surface which lies close to saddle points in a generic 2D dispersion associated with the $(CuO_2)_n$ layers, at least for Hg-1212 and Hg-1223.[34] Normal-state transport measurements have provided corroborating evidence for this picture, showing a highly 2D electrical resistivity ($\rho_c \gg \rho_{ab}$) and such characteristic anomalies as linear temperature dependence of the in-plane resistivity ($\rho_{ab} \propto T$), non-Drude temperature dependence of the Hall angle ($\cot\theta_H \propto T^2$), pressure dependence of T_c and doping-sensitive thermopower,[35,36] all of which could be regarded as generic effects of the band structure.[22,37–40] Preliminary tricrystal experiments on the Hg-1212 films have also demonstrated the signature of d-wave pairing symmetry.[17] These results strongly suggest that the Hg cuprates can be modeled in the combined d-wave 2D van Hove scenario.

Mixed tunneling data have been reported on the Hg cuprates so far. Chen *et al.* observed BCS-like spectra with near-BCS gap values in polycrystalline Hg-1201 by point-contact spectroscopy.[41] Jeong *et al.*, observed two types of spectra, one BCS-like with a large gap and the other showing heavily smeared double-gap features, in polycrystalline Hg-1223 by scanning tunneling spectroscopy (STS).[42] Rossel *et al.* also observed smeared gap spectra by STS in melted polycrystalline Hg-1223, but enhanced-peak spectra with very large gap values in single crystals of Pb-doped Hg-1234.[43] Differences in sample quality and measurement technique could have contributed to this spectral variety. In each case a specific set of model assumptions was used to analyze the data, but entirely within the conventional framework of an s-wave energy gap and without consideration of the band structure.

This paper presents tunneling measurements by scanning tunneling spectroscopy on epitaxial films of Hg-1212 and polycrystalline samples of Hg-1201 and Hg-1223. The Hg-1212 data is, as far as we know, the first of its kind, and all the tunneling spectra were taken with the same measurement technique. The spectra show distinctively non-BCS gap behaviors which cannot be easily reconciled with the standard s-wave model. We explain the data by explicitly considering quasiparticle tunneling in the d-wave 2D van Hove scenario, using a traditional planar-junction formalism for elastic and specular transmission. Model calculations based on these generic assumptions reveal a profoundly directional and energy-dependent spectral weighting due to the gap anisotropy and $\mathbf{k}$ dependence of the matrix element $|T|^2$. Tunneling across a c-axis junction is shown to cause spectral enhancement, while tunneling across an a-axis junction leads to spectral suppression and thereby a quasilinear spectral background. Simple superposition of these two model cases enables an interpretation of our data. The analysis indicates very large values for the d-wave energy-gap maximum: $\Delta_0 \approx 33$, 50, and 75 meV for optimally doped Hg-1201, Hg-1212, and Hg-1223, respectively, corresponding to reduced-gap ratios of $2\Delta_0/k_BT_c \approx 7.9$, 9.5, and 13. These large reduced-gap ratios deviate markedly from BCS universality, and suggest an overall trend of $2\Delta_0/k_BT_c$ rising with T_c among the cuprates.

The experimental procedure is described in Sec. II. The spectroscopy data is presented in Sec. III, then analyzed in Sec. IV. The full d-wave 2D van Hove model for quasiparticle tunneling is given in Sec. V, along with model calculations simulating various junction orientations. The simulations are used to interpret the data and determine the d-wave gap values in Sec. VI.

II. EXPERIMENT

Samples of optimally doped Hg-1201, Hg-1212, and Hg-1223 were used in our experiment. Epitaxial c-axis films of Hg-1212 were made by pulsed laser-ablated deposition on (100) $SrTiO_3$ substrates,[44] showing sharp resistive and diamagnetic transitions at ~ 123 K, with zero resistivity at ~ 122 K and a room temperature resistivity of $\sim 400\ \mu\Omega$ cm. Polycrystalline samples of Hg-1201 and Hg-1223 were synthesized by a controlled vapor/solid reaction technique,[33] showing similarly sharp T_c's at ~ 97 and ~ 135 K, respectively, with room-temperature resistivities ~ 20 mΩ cm. X-Ray diffraction verified all the samples to be single-phase and the film samples to be have high crys-

talline alignment. Tunneling spectroscopy was performed with a cryogenic scanning tunneling microscope (STM) at 4.2 K in ~ 1 μTorr of helium exchange gas, using a platinum tip as counter-electrode. Details of the STM is published elsewhere.[45] To prevent surface degradation by the atmosphere, each sample was kept under dry argon prior to being loaded for measurement. Stable tunneling junctions were formed between the voltage-biased sample and piezo-driven tip in constant-current feedback mode. Current vs voltage I-V spectra were taken by momentarily disabling the STM feedback at a fixed spot on a sample and rapidly sweeping the voltage (~ 1 mV/0.1 ms) while measuring the current. This process was repeated 256 times in rapid succession to average the I-V data. Conductance dI/dV spectra were extracted by numerically differentiating the I-V spectra. Constant-current topography was attempted but did not produce meaningful images. The scanning capability did allow spectroscopy to be performed over large areas ($\sim 1 \times 1$ μm^2) as a check of spectral reproducibility. Junction quality was monitored by checking the effective barrier height ϕ (in eV) according to the standard relation $I \propto e^{-\sqrt{\phi}s}$ between piezo displacement s (in Å) and tunneling current. Very low values for ϕ (~ 1 meV) were typically observed, indicating tip-sample contact and the existence of a dead layer acting as tunnel barrier. Large values ($\phi \sim 2.5$ eV) were occasionally observed, as instances of ideal ''vacuum-gap'' junction. No correlation was noticed between the apparent junction quality and spectral behavior. All the spectra presented here were taken on low-transmission junctions (~ 10 to 100 MΩ), i.e., well in the normal-metal–insulator–superconductor (NIS) Giaever tunneling regime where NS Andreev reflection probability is low.[46]

III. SPECTROSCOPY DATA

Conductance dI/dV spectra showing distinct gap features were observed. Representative spectra of this kind are shown in Figs. 1(a), 1(b), and 1(c) for Hg-1201, Hg-1212, and Hg-1223, respectively, with the insets displaying the current-voltage I-V characteristics. These spectra were reproducible over large areas ($\sim 0.1 \times 0.1$ μm^2) in each sample, and insensitive to either the tunneling distance (for vacuum-gap junctions) or tip pressure (for contact junctions) as controlled by the feedback current. Pronounced spectral peaks appear at $\sim \pm 33$, ± 50, and ± 75 meV, respectively for Hg-1201, Hg-1212, and Hg-1223. The peak shapes are fairly broad and symmetric, and the peak heights are generally asymmetric about zero-bias, except for Hg-1201. A small zero-bias conductance ($<10\%$ of peak height) is present, and the midgap behavior shows some variation, being more rounded for the Hg-1212 films and sharper for Hg-1223. Quasilinear backgrounds exist in all the spectra and are generally asymmetric in slope about zero bias, again with the exception of Hg-1201. Apart from the quasilinear background, these spectra look very similar to the c-axis STM spectra taken on $Bi_2Sr_2CaCu_2O_{8+\delta}$ (BSCCO) crystals by Renner *et al.*[47] and by Boon *et al.*[48] In our spectra, small high-voltage kink structures are visible for Hg-1201, and a dip structure is visible for Hg-1223 just above the gap on the negative-bias side. An analysis of these above-gap structures is beyond the scope of this paper. However, it is noteworthy that the dip structure has also been observed in tunneling and ARPES spectra on BSCCO and attributed to quasiparticle retardation in the context of d-wave pairing symmetry.[49]

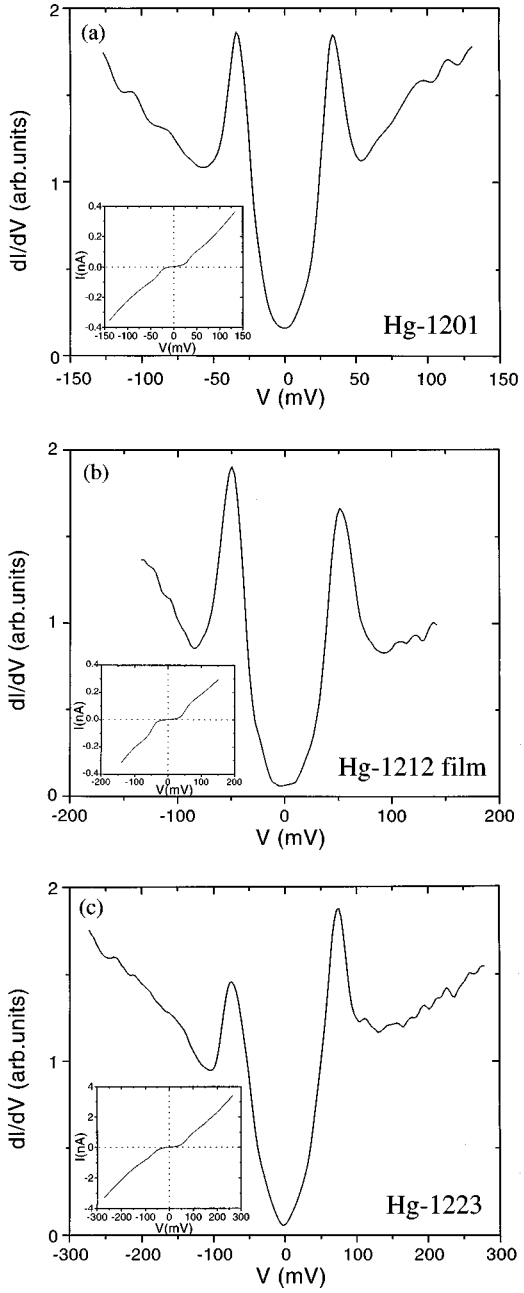

FIG. 1. Tunneling conductance spectra showing distinct gap features, taken at 4.2 K with a Pt tip by STM: (a) polycrystalline Hg-1201, with $T_c \approx 97$ K; (b) epitaxial c-axis film of Hg-1212, with $T_c \approx 123$ K; (c) polycrystalline Hg-1223, with $T_c \approx 135$ K. The insets display the corresponding current-voltage characteristics. The voltage corresponds to bias of the sample relative to the tip.

For the polycrystalline samples, two other types of spectra were also observed. The first type shows a pronounced zero-bias conductance peak (ZBCP). A typical example, taken on Hg-1201, is given in Fig. 2. Such spectra have often been observed in the high-T_c cuprates, particularly on {110} tunnel junctions, i.e., with the junction oriented normal to a $k_x = \pm k_y$ crystalline axis in the ab plane.[50] The ZBCP has been attributed to midgap surface states on a junction oriented

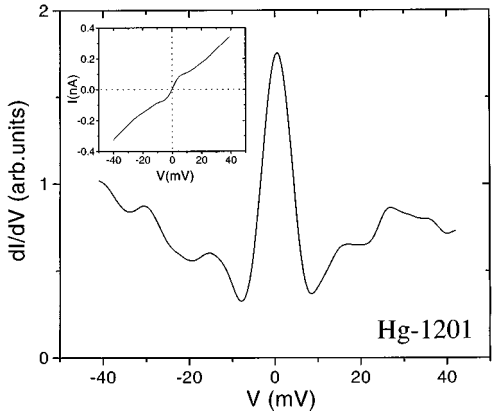

FIG. 2. Example of tunneling spectra showing zero-bias conductance peak (ZBCP), taken with a Pt tip at 4.2 K on polycrystalline Hg-1201 ($T_c \approx 97$ K). The main plot displays the conductance data, and the inset gives the corresponding current-voltage characteristic.

along or near a gap-node axis of a *d*-wave superconductor, and could thus be considered a signature of $d_{x^2-y^2}$ order parameter symmetry as well as other symmetries with phase sign changes.[51–54] This issue will be discussed in Sec. V. The other type of spectra shows heavily suppressed gap features. A typical example, taken on Hg-1223, is given in Fig. 3. Such suppressed-peak spectra are commonly observed in the high-T_c cuprates.[4–6] The absence of clear gap peaks, together with steep quasilinear background and smeared subgap behavior, can be regarded as generic anomalies which tend to complicate spectral analysis. Several groups have investigated the quasilinear conductance background. Hartge *et al.*, for example, have offered an explanation of the background in terms of out-of-plane tunneling.[16] However, even if the background were subtracted out or normalized away, smearing parameters much larger than the thermal broadening at 4.2 K would still be needed to fit the BCS density of states, thus making the gap determination highly uncertain. Kirtley has addressed this issue by weighting the BCS density of states $N(E,\Delta)=E/\sqrt{E^2-\Delta^2}$ with a Gaussian gap distribution,[7] to account for the possibility of chemical inhomogeneity of the tunneling surface. An alternative mechanism for the spectral smearing was proposed by van Bentum

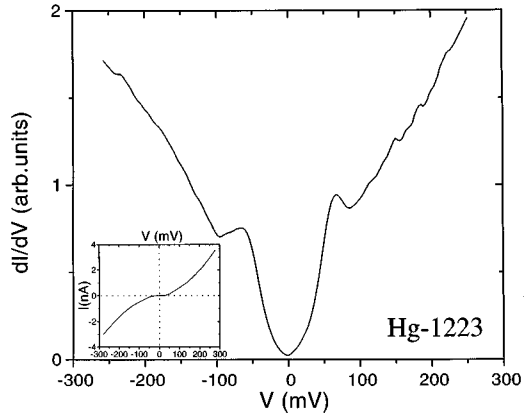

FIG. 3. Example of tunneling spectra showing suppressed gap features, taken at 4.2 K with a Pt tip on polycrystalline Hg-1223 ($T_c \approx 135$ K). The main plot displays the conductance data, and the inset gives the corresponding current-voltage characteristic.

et al.,[8] by considering energy-fluctuation effects associated with tip-sample charging through single-electron tunneling.[55–57] Although plausible, the Gaussian distribution and charge-fluctuation models can only account for peak suppression and not at all for peak enhancement. As will be shown in Sec. V, a combined consideration of the band structure and gap symmetry can explain both types of spectral behavior rather naturally. In the following section (Sec. IV), exclusive focus will be given to the enhanced-peak spectra (Fig. 1) which are more amenable to spectral analysis and gap determination.

IV. SPECTRAL ANALYSIS

s-wave. Conventional analysis of quasiparticle tunneling between a metal electrode and a superconductor relies on the Giaever expression for normalized conductance[58]

$$\frac{(dI/dV)_s}{(dI/dV)_n}=\int_{-\infty}^{\infty} N_s(E)\,\frac{-\partial F(E+eV)}{\partial(eV)}\,dE, \qquad (1)$$

where the subscripts *s* and *n* denote superconducting state and normal state in the superconductor, E is the quasiparticle energy defined relative to the Fermi level, $F(E)=[1+\exp(E/k_BT)]^{-1}$ is the Fermi function, and the BCS quasiparticle density of states is written in the Dynes form[59]

$$N_s(E)=\mathrm{Re}[|E-i\Gamma|/\sqrt{(E-i\Gamma)^2-\Delta^2}], \qquad (2)$$

with Γ as a smearing parameter to account for quasiparticle lifetime. Note that this expression presupposes an *s*-wave energy gap Δ and is completely insensitive to band structure. The superconductor is implicitly assumed to be an isotropic metal with simple dispersion, thus allowing the tunneling transition probability $|T|^2$ to be factored out of the integral as a constant within the domain of interest and normalized away.

An attempt was made to fit this model to the measured dI/dV spectra shown in Fig. 1. The normal-state conductance $(dI/dV)_n$ was estimated by interpolating the spectral background with polynomial regression. The Fermi function was set to $T=4.2$ K which provided negligible (~ 1.3 meV) thermal smearing. Fitting results from the data for Hg-1201 are presented as an example in Fig. 4(a). The data is given by the crosses and the fits indicated by lines. Only the positive-bias branch is shown for the sake of clarity. Despite the well-developed gap features and the adjustable smearing parameter, spectral agreement between data and model is poor. Peak height and gap bottom could not both be satisfied with a single choice of Γ. As shown by the two trial fits in Fig. 4(a), the model curve is either too ''short'' or too ''low'' and inevitably lopsided. This dilemma was also encountered by Renner *et al.*[47] and by Boon *et al.*[48] in their analysis of *c*-axis tunneling data taken on cold-cleaved BSCCO crystals. The measured peak-shape is clearly more symmetric than the form of $N_s(E)$ would allow.

It is important to note that since the BCS square-root singularities are asymptotic in form, they tend to broaden asymmetrically about $\pm\Delta$ with the energy-smearing associated with $i\Gamma$ and shift the spectral peaks outwards. The same

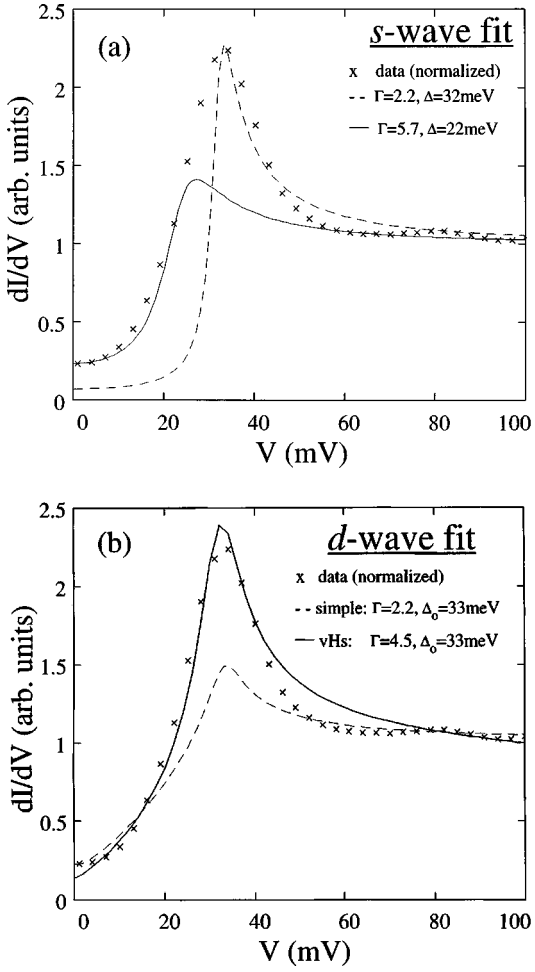

FIG. 4. Fitting results of the normalized Hg-1201 data from Fig. 1(a). Only the positive-bias branch is shown for comparison, with the data given by the cross-symbols. (a) s-wave model, using the BCS density of states $N_s = E/\sqrt{E^2-\Delta^2}$ with lifetime broadening Γ as an adjustable parameter. Peak height and gap bottom could not both be satisfied with a single choice of Γ. The fit is either too ''short'' (solid curve) or too ''low'' (dotted curve) and inevitably ''lopsided,'' demonstrating the incompatibility of N_s with the data. (b) d-wave models: dotted curve represents the simple angle-averaged N_s, using the simplified gap function $\Delta = \Delta_0 \cos(2\varphi)$; solid curve represents the vHs-enhanced d-wave quasiparticle DOS, using the gap function $\Delta_{\mathbf{k}} = \Delta_0(\cos k_x - \cos k_y)/2$ and the dispersion $\varepsilon_{\mathbf{k}} = -2t(\cos k_x + \cos k_y)$. Good spectral agreement between the data and the latter d-wave model demonstrates the importance of the band structure.

argument would also apply to either thermal, Gaussian, or charge-fluctuation broadening. If the smearing is large, this shift can amount to a sizable discrepancy between the apparent peak position and the fitting parameter Δ. Γ/Δ ratios as large as $\sim 50\%$ have been reported in some instances, making the gap determination highly uncertain.[4–6] In our fitting of the Hg-1201 data, Δ can range anywhere between 22 and 33 meV, the former requiring a large lifetime parameter $\Gamma/\Delta \approx 25\%$. This large margin of uncertainty indicates a fundamental incompatibility between our data and the s-wave model.

Simple d wave. A simple d-wave fit was also attempted, using a heuristic model given by Won and Maki.[60] This model assumes the tunneling to sample uniformly all directions in the ab plane, by angle averaging the quasiparticle DOS $N_s(E,\Delta)$ with a simplified d-wave energy-gap function,

$$\Delta(\mathbf{k}) = \Delta_0 \cos(2\varphi), \tag{3}$$

where Δ_0 is the gap maximum and φ is the polar angle in $\mathbf{k}$ space. The averaging scheme is plausible for a junction with large contact area and nonuniform orientation, but invariably neglects the band structure by normalizing away the tunneling matrix element $|T|^2$. The nodal gap function provides a distribution of gap values which effectively broadens the gap singularity. This implies a peak shape which is more symmetric than the s wave model and in principle more compatible with the data. Typical results of the fit are shown as dashed curves in Fig. 4(b), again using the Hg-1201 data as an illustrative example. Although relying less on lifetime smearing ($\Gamma/\Delta_0 \approx 7\%$) than the s-wave fit to accommodate the subgap behavior, the simple d-wave fit is also poor. The nodal d-wave symmetry effectively shifts much of the spectral weight inward, but at the expense of the peak height. This basic inadequacy suggests that the quasiparticle DOS assumed by this d-wave model is still too simple.

vHs-enhanced d wave. Next we consider how the band structure alters the d-wave quasiparticle DOS. A convenient expression for calculating the quasiparticle DOS at zero temperature is

$$N_s(E) = \sum_{\mathbf{k}} \delta(E - \sqrt{\xi_{\mathbf{k}}^2 + \Delta_{\mathbf{k}}^2}), \tag{4}$$

where $\Delta_{\mathbf{k}}$ is the superconducting energy gap and $\xi_{\mathbf{k}}$ is the normal-state energy dispersion defined relative to the Fermi level. For the high-T_c cuprates, it is justified on both theoretical and experimental grounds[17–22] to assume

$$\Delta_{\mathbf{k}} = \Delta_0(\cos k_x - \cos k_y)/2 \tag{5}$$

for a $d_{x^2-y^2}$ pairing symmetry, and to use the 2D tight-binding dispersion

$$\xi_{\mathbf{k}} = -2t(\cos k_x + \cos k_y) + 4t'(\cos k_x \cos k_y) - \mu \tag{6}$$

to model the Cu-O square lattice, where the pairing interaction is presumably located. Here μ is the Fermi energy, while t and t' represent the nearest-neighbor and next-nearest-neighbor overlap integrals. The presence of saddle points at $\mathbf{X}$ and $\mathbf{Y}$ in the Brillouin zone (BZ) gives rise to a logarithmic singularity (the 2D vHs) near the Fermi level, and the next-nearest-neighbor term t' has the effect of denesting the FS from half filling.

The main effect of the vHs on the quasiparticle DOS is to enhance the height of the gap singularity, which is broadened by the d-wave gap anisotropy. Intuitively speaking, as the energy gap opens up about the vHs, more states must now pile up on the gap edges than for a flat energy band. This enhancement mostly affects states near the saddle points, where heightened DOS ($\sim \partial k/\partial \xi \to \infty$) coincides with maxima in the d-wave gap distribution. The larger gap-values receive heavier spectral weighting in summing over the BZ, leading to a peak shape which is a convolution of the BCS square-root singularity and the logarithmic van Hove singularity. The vHs-enhanced d-wave peak is both broader

than the s-wave peak and taller than the simple d-wave peak, exactly as required to fit our data. To demonstrate this, the background-normalized Hg-1201 data was fitted to the vHs-enhanced d-wave DOS, using Eq. (4) with the band-structure parameters $t=185$ meV and $\mu=0.5$ eV, the δ function represented by a Lorentzian of width Γ and the energy E replaced by the voltage V. Here, the band asymmetry is implicitly ignored by setting $t'=0$ and will be explicitly considered in Sec. V. A typical fit in arbitrary units is included as the solid curve in Fig. 4(b). The spectral agreement is quite good, with some minor midgap and above-gap discrepancies, and a moderate lifetime parameter ($\Gamma/\Delta_0 \approx 12\%$). It is interesting to note that a similar spectral resemblence was noticed in the analysis of c-axis STM spectra taken on BSCCO by Renner and co-workers.[47]

It should be emphasized here that the *quasiparticle density of states* cannot be directly equated with the *tunneling conductance*. They are distinct spectra related by the tunneling matrix element $|T|^2$ according to the transfer-Hamiltonian formalism.[61] In fact, according to the well-known argument by Harrison,[30] any band-structure information contained in the former is not expected to carry over to the latter, because of cancellation between the bare DOS ($\sim \partial k/\partial \xi$) and a group velocity factor ($\sim \partial \xi/\partial k$) inherent in $|T|^2$. For our band structure, the vHs which alters the quasiparticle DOS should in principle be offset by group velocity suppression near the saddle points and not survive the tunneling. Therefore, any manifestation of the vHs in the tunneling spectra needs to rigorously justified. Strictly speaking, the cancellation argument is only exact for specular tunneling (transverse momentum conserved) into an isotropic material with simple parabolic dispersion, and could break down if the junction is diffusive[62] or if the band structure is sufficiently complex.[1,30] For the latter case, $|T|^2$ can become significantly energy and **k** dependent and no longer removable from the tunneling integral. This essentially invalidates the background normalization procedure, making the spectral analysis highly nontrivial. Still, the good spectral agreement seen in Fig. 4(b) suggests a basic compatibility between the data and the vHs-enhanced d-wave model. To understand this we must explicitly consider how $|T|^2$ relates the calculated quasiparticle DOS with the tunneling conductance observed.

V. QUASIPARTICLE TUNNELING IN THE d-WAVE 2D VAN HOVE SCENARIO

Model. We start with the general expression for quasiparticle tunneling across a normal-metal–insulator–superconductor (NIS) junction at zero temperature, derived from many-body formalism:[64]

$$I=\pm 2\pi e\sum_{\mathbf{k}\cdot\mathbf{q}} |T_{\mathbf{kq}}|^2[1\mp\xi_{\mathbf{k}}/E_{\mathbf{k}}]\delta(\xi_{\mathbf{q}}-eV\pm E_{\mathbf{k}}) \times\theta(|eV|-E_{\mathbf{k}}). \tag{7}$$

Here I is the current (per junction area) and V is the voltage, with the $\pm$ sign indicating its polarity (S relative to N). The subscripts **k** and **q** label the wave vectors for S and N. The step function θ represents the Fermi function at zero temperature, and the delta-function δ reflects energy-conservation (elastic tunneling). For the superconductor, the quasiparticle and normal-state dispersions $E_{\mathbf{k}}$ and $\xi_{\mathbf{k}}$ are related by the gap function $\Delta_{\mathbf{k}}$ according to $E_{\mathbf{k}}{}^2=\xi_{\mathbf{k}}{}^2+\Delta_{\mathbf{k}}{}^2$. For the metal electrode, a free-electron dispersion $\xi_{\mathbf{q}}=\hbar^2q^2/2m$ is assumed. In the planar-junction approximation, the transmission becomes a one-dimensional problem (longitudinal along $\hat{x}$) with the simple tunneling matrix element derived from the transfer-Hamiltonian formalism:[1]

$$|T_{\mathbf{kq}}|^2=\frac{\partial\xi_{\mathbf{k}}}{\partial k_L}\frac{\partial\xi_{\mathbf{q}}}{\partial q_L}D(\varepsilon_L)\delta(k_T-q_T). \tag{8}$$

Here, the subscripts L and T indicate directions longitudinal and transverse to the junction, the δ function indicates conservation of transverse momentum (specular transmission), and the barrier transmission is given by the semiclassical expression[1,29]

$$D(\varepsilon_L)=g\exp\left(-2\int_0^d\kappa dx\right), \tag{9}$$

where the longitudinal energy $\varepsilon_L=E_k-\hbar^2k_T^2/2m$ according to the assumptions of elasticity and specularity, and $\kappa=\sqrt{2m[U(x,V)-\varepsilon_L]/\hbar^2}$ is the wave vector inside the barrier of height $U(x,V)$, thickness d, and free-electron mass m. Assuming a square barrier in the low-transmission limit $e^{-2\kappa d}\ll 1$, the prefactor g can be written as[1,30]

$$g=\frac{16q_L\kappa^2k_L}{(q_L{}^2+\kappa^2)(\kappa^2+k_L{}^2)} \tag{10}$$

to represent wave vector matching across the NIS junction. These expressions are exact for specular transmission across a planar junction within the elastic channel. Note that if $|T_{\mathbf{kq}}|^2$ is set to unity, Eq. (7) can be differentiated with respect to voltage to recover Giaever's expression for quasiparticle DOS [Eq. (1)], apart from the $1\mp\xi_{\mathbf{k}}/E_{\mathbf{k}}$ factor which is essentially the occupation probability reflecting the mixed electron/hole character of a quasiparticle.[65]

In the conventional scenario based on an s-wave energy gap and free-electron dispersions, the tunneling equation is simplified in the continuum limit by the following arguments.

(1) The group velocity factors eliminate the longitudinal band structures in converting the integrals over longitudinal momenta to integrals over energy; e.g., $\partial\xi/\partial k_L$ cancels with $\partial k_L/\partial\xi$, which is a Jacobian in the coordinate-transformation $dk_L\rightarrow d\xi$.[30]

(2) The barrier transmission factor $D(\varepsilon_L)$ collapses the transverse momentum integration by falling off rapidly with k_T or q_T, i.e., narrow tunneling cone, thereby suppressing the transverse band structure.[66,67]

(3) The wave vector matching prefactor g is set to unity by invoking the WKB approximation, which is valid for junction interfaces sufficiently gradual compared with the electron wavelength.[29,30]

(4) The coherence factor $1\mp\xi_{\mathbf{k}}/E_{\mathbf{k}}$ is set to unity, because $\xi_{\mathbf{k}}/E_{\mathbf{k}}$ is odd about the Fermi surface, i.e., electron-hole symmetry.

Equation (7) then becomes $I=\pm C\int_{-\infty}^{\infty}d\xi\,\theta(|eV|-E)D(E)$, where the collapsed k_T integral, an uninteresting

$\xi_{\mathbf{q}}$ integral, and all the numerical factors have been absorbed into the constant C. Assuming $D(E)$ to be weak and making the variable transformation $d\varepsilon \rightarrow dE$, this expression can be differentiated to recover the conventional expression Eq. (1) in the zero-temperature limit. Note that the tunneling dI/dV spectra here does not measure the superconductor's normal-state DOS, but only the quasiparticle DOS $E/\sqrt{E^2-\Delta^2}$ which is just the Jacobian $\partial\xi/\partial E$. This is a well-known realization of the principle that tunneling is insensitive to any *bare* DOS based on an independent-particle dispersion, but does directly reveal any *dressed* DOS ''renormalized'' by many-body effects.[68]

In the d-wave 2D van Hove scenario, this conventional simplification is generally not possible. Each of the last three arguments can break down as a consequence of the band structure. These possibilities will be discussed in the context of c-axis tunneling, a-axis tunneling, and band-structure asymmetry below. As a preliminary remark, it is important to point out that despite a quasi-2D band structure the probability for c-axis tunneling (junction perpendicular to the c axis) cannot be ignored. This is a natural but counterintuitive consequence of the band-structure cancellation argument. Essentially, since the longitudinal band structure drops out of the problem, a flat c-axis dispersion cannot suppress tunneling across a c-axis junction as in a usual transport process, which scales inversely with the effective mass. For an open energy contour such as a cylindrical FS, a low c-axis group velocity ($\sim\partial\xi/\partial k_L$) also implies a large degeneracy of states ($\sim\partial k_L/\partial\xi$), and the two factors would then offset each other. This effectively removes the effective mass from the tunneling problem, as is clear from Eq. (7). Therefore, even if the c-axis conductivity is low (e.g., $\sigma_a/\sigma_{ab}\sim 10^{-4}$ according to Ref. 35) c-axis tunneling could still be appreciable. Note that here we are referring to tunneling *into* a 2D system based on Cu-O planes, and make no assumptions about any tunneling *between* the planes.

First, it is not difficult to see that the highly idealized tunneling cone argument breaks down for a c-axis junction in the 2D scenario. For a simple FS and a square barrier of height U_0 and thickness d, the transmission probability Eq. (9) can be expanded into a Gaussian, $D(\varepsilon_L)\sim \exp(-\beta k_T^2)$, where $\beta=\hbar d/\sqrt{2mU_0}$. For typical barrier parameters ($d=10$ Å, $U_0=1$ eV) this Gaussian is quite sharp ($\beta\approx 50$), collimating the tunneling within a narrow momentum-cone ($\Delta\varphi\approx 8°$) from the junction normal.[66,67] In general, however, the tunneling cone width could vary with local FS curvature, depending on how k_T relates with k_φ in the $\xi_{\mathbf{k}}$ contour. For an open energy contour, such as along the axis of a cylindrical FS given by $\xi_{\mathbf{k}}=(\hbar^2/2m)(k_x^2+k_y^2)$, the radial k_T becomes independent of the azimuthal k_φ. This is essentially the geometry for a c-axis junction in our 2D scenario. The tunneling cone can be said to ''flatten out,'' as the longitudinal energy ($\varepsilon_L=E_{\mathbf{k}}-\hbar^2k_T^2/2m$) in the barrier and therefore $D(\varepsilon_L)$ become invariant over a given energy contour, apart from a small difference between $E_{\mathbf{k}}$ and $\xi_{\mathbf{k}}$. Without loss of generality ε_L can be set to a constant, making $D(\varepsilon_L)$ uniform in energy. This uniform weighting leads to full survival of the transverse band structure through the Jacobian $\partial k_T/\partial\xi$ which, unlike the longitudinal band structure, is not cancelled by any reciprocal factors in the matrix element $|T|^2$ upon integration over energy. The tunneling conductance dI/dV should therefore be directly proportional to the 2D DOS lying transverse (in the ab plane) to the junction normal (c axis). In the literature this corresponds to a well-known *final-state effect*, first observed by tunneling into Landau-levels of electronic states localized on a semiconductor surface, which fully manifests the quantized transverse 2D band structure.[1,69,70] In our model case of a 2D superconductor, the vHs-enhanced quasiparticle DOS is expected to show up in c-axis tunneling.

Second, the WKB approximation becomes invalid when the energy dispersion $\xi_{\mathbf{k}}$ goes through an extremum along the direction normal to the tunneling junction.[71,72] For the cuprates, the situation corresponds to a-axis tunneling (junction perpendicular to the a axis) in the vicinity of the saddle point at $\mathbf{X}$. As was shown by van Bentum and Tsuei for the case of a-axis tunneling in the 2D van Hove scenario,[73] the longitudinal wave vector k_L is effectively rescaled relative to the BZ edge, in accordance with the effective mass method.[74] This rescaling causes the WKB coefficient g to vanish continuously as the BZ edge is approached, i.e., $g\rightarrow 0$ as $k_L\rightarrow 0$ according to Eq. (10), signifying severe wave vector mismatch across the junction and diminished barrier transmission. In the WKB picture, a vanishing wave vector represents an extremely large electron wavelength λ compared with the length scale δx of the potential jump at the insulator-cuprate interface.[29,30] The WKB approximation breaks down because the gradual-junction criterion $\lambda \ll \delta x$ is no longer satisfied. As will be demonstrated in the simulations below, this breakdown makes the tunneling probability highly energy dependent, producing a V-shaped spectral weighting which suppresses the gap singularities and gives rise to a quasilinear conductance background (see Fig. 5).

Finally, the coherence factor $1\mp\xi_{\mathbf{k}}/E_{\mathbf{k}}$ cannot be ignored if electron-hole symmetry about the Fermi surface is broken. For our 2D tight-binding band [Eq. (6)] this happens because the FS is denested from half filling by t'. This asymmetry corresponds to uneven quasiparticle occupation probability $\frac{1}{2}[1\mp\xi_{\mathbf{k}}/E_{\mathbf{k}}]$ above and below the energy gap. In essence the term $\xi_{\mathbf{k}}/E_{\mathbf{k}}$ is no longer odd in $\mathbf{k}$ about $\xi_{\mathbf{k}}=0$ and does not cancel out upon summation [Eq. (7)] over the entire band. This vestige of the $\xi_{\mathbf{k}}/E_{\mathbf{k}}$ term is expected to produce spectral asymmetry about zero bias in tunneling, as implied by the $\mp$ sign. It could also introduce considerable directional weighting, by virtue of the anisotropies inherent in both $\xi_{\mathbf{k}}$ and $\Delta_{\mathbf{k}}$. Such a weighting may be quite nontrivial in the d-wave 2D van Hove scenario, considering for example that $\xi_{\mathbf{k}}/E_{\mathbf{k}}$ is unity along the gap nodes but varies with the energy in the saddle point directions. In our model calculations this anisotropy turns out to be small and only the spectral asymmetry is appreciable, although both effects could become important as the band asymmetry increases with larger t'.

Simulations. To demonstrate quasiparticle tunneling in the d-wave 2D van Hove scenario, model calculations of the full tunneling equation [Eq. (7)] were performed, using the 2D tight-binding band dispersion [Eq. (6)] and the d-wave gap function [Eq. (5)]. Finite temperature was introduced by representing the step function as a Fermi function at temperature T. Finite quasiparticle lifetime was included by expressing the δ function as a Lorentzian of width Γ. The following

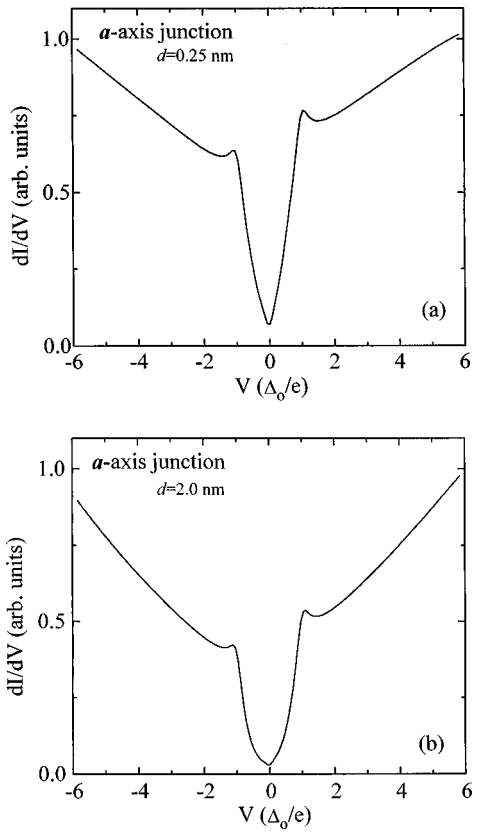

FIG. 5. Simulations of quasiparticle tunneling for an a-axis junction in the d-wave 2D van Hove scenario: (a) for a thin junction ($d=0.25$ nm); (b) for a thick junction ($d=2.0$ nm). Note the spectral suppression, smearing and asymmetry, which are generic anomalies seen in the high-T_c cuprates (cf. Fig. 3).

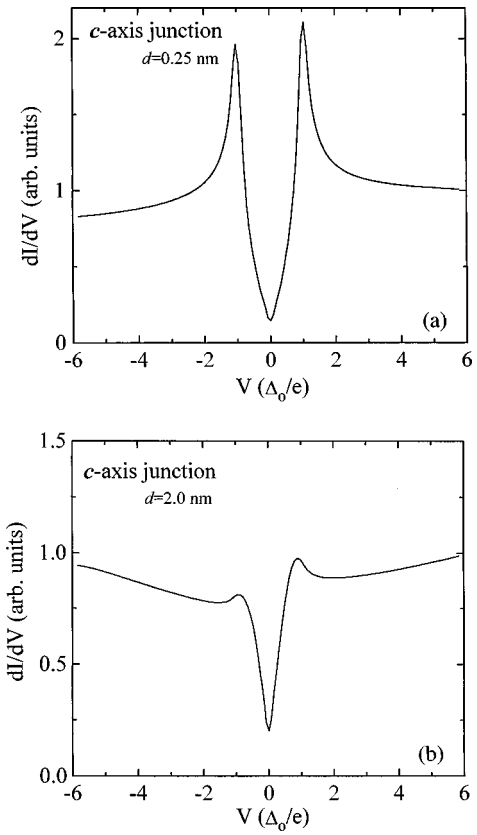

FIG. 6. Simulations of quasiparticle tunneling for a c-axis junction in the d-wave 2D van Hove scenario: (a) for a thin junction ($d=0.25$ nm); (b) for a thick junction ($d=2.0$ nm). Note the spectral enhancement in (a), which is essentially the vHs-enhanced d-wave quasiparticle DOS [cf. Fig. 4(b)].

model parameters were used: $t'=0.16t$, $\mu=2.7t$, $\Delta_0=0.1t$, $\Gamma=0.02t$, and $k_BT=0.002t$. The band-structure parameters correspond to a doping level of $\sim 15\%$ with the vHS exactly at μ. For the transmission probability $D(\varepsilon_L)$, a symmetric trapezoidal barrier $U(V)=U_0-\frac{1}{2}|eV|$ was assumed for simplicity, with a large height $U_0=1.5$ eV to minimize the voltage dependence. The Fermi energies were taken to be 0.5 eV for the cuprate and 2.5 eV for the metal. The in-plane Cu-O lattice parameter $a=3.9$ Å was used to set the scale of the wave vector $\mathbf{k}$. Two values for the barrier thickness, $d=2.5$ and 20 Å, were selected for comparison.

Conductance dI/dV spectra simulating an a-axis junction and a c-axis junction are shown respectively in Figs. 5 and 6 in normalized units (arbitrary vs Δ_0/e). These spectra will be described and interpreted in the following. First, the a-axis junction spectra (Fig. 5) show heavily suppressed gap peaks at $\sim\pm\Delta_0/e$, a steep quasilinear background, asymmetry about zero bias, appreciable subgap smearing, and a small midgap conductance. The thin-junction ($d=2.5$ Å) case looks remarkably similar to the suppressed-peak type of spectra shown as data in Fig. 3 (Sec. III). As discussed above, the peak suppression and quasilinear background are due to a V-shaped spectral weighting associated with breakdown of the WKB approximation near the saddle point **X** where the FS touches the BZ edge. The spectral asymmetry reflects band asymmetry about the FS which is denested by the next-nearest-neighbor interaction t'. The zero-bias conductance, on the other hand, can be understood as available states introduced by the temperature and lifetime broadening. And the subgap smearing can be attributed to an appreciable tunneling cone width which is sensitive to the barrier thickness ($\beta\propto d$) and to the local FS curvature. Decreasing the barrier thickness effectively widens the tunneling cone (smaller β), which explains why there is more subgap smearing for the thinner junction [Fig. 5(a)]. Increasing the barrier thickness, however, tends to amplify the voltage dependence $U(V)$ implicit in $D(\varepsilon_L)$, thus accounting for the additional spectral slope for the thicker junction [Fig. 5(b)]. No clear gap features show up in either case.

The c-axis junction simulations show a very different spectral behavior which is extremely sensitive to the barrier thickness. The thin-junction result [Fig. 6(a)] has pronounced but broadened gap peaks at $\pm\Delta_0$, with a very small midgap conductance, no noticeable background slope, and overall asymmetry favoring positive bias. This is essentially the vHs-enhanced d-wave quasiparticle DOS we expected, as the tunneling cone flattens out with the geometry to reveal the 2D band structure transverse to the junction normal. The spectral asymmetry follows from the band structure asymmetry which shows up through the coherence factor. WKB breakdown effects do not apply here, since the longitudinal wave vector k_L does not cross the BZ edge. The thick-junction result [Fig. 6(b)], on the other hand, shows dull peaks with considerable subgap smearing and a larger zero-bias conductance. This behavior can be understood in terms of the cross-shaped FS shape, which introduces a polar-angle

weighting through k_T in the transmission probability $D(\varepsilon_L) \sim \exp(-\beta k_T^2)$. Since k_T is smallest along the $k_x = \pm k_y$ direction for this geometry, this weighting favors the gap nodes over the gap maxima and, for a sufficiently thick barrier (because $\beta \propto d$), counters the vHs enhancement which has essentially the opposite weighting. Subgap smearing and zero-bias conductance follow naturally, since the smaller gaps are more susceptible to the thermal and lifetime broadening. A mild spectral slope can also arise [Fig. 6(b)], as the larger barrier thickness enhances the voltage-dependence implicit in $D(\varepsilon_L)$. It is important to note that these effects are negligible for the thin barrier case, i.e., $D(\varepsilon_L) \rightarrow 1$ in the limit $d \rightarrow 0$ and the tunneling conductance essentially becomes the full quasiparticle DOS.

Another model case of interest is the ''nodal'' {110} junction, i.e., with the junction normal oriented along a nodal axis of the $d_{x^2-y^2}$ order parameter. Hu and co-workers[51] as well as Tanaka and co-workers[52] have considered this nodal junction and, more generally, nonantinodal junction scenarios theoretically, using the Bogliubov-deGennes equations[63] and the formalism of Blonder, Tinkham, and Klapwijk.[46] Their simulations demonstrate the existence of a midgap surface state which can give rise to a zero-bias conductance peak (ZBCP) in the tunneling spectra. As mentioned in Sec. II, such spectra have been observed in our polycrystalling Hg-cuprate samples [Fig. (2)], as well as by previous workers in other cuprates, particularly on {110} tunnel junctions.[50] We will examine the appearance of the ZBCP experimentally in a separate paper involving controlled *in-plane* junctions.[54] Here it suffices to remark that since the nodal axis lies far away from the saddle points, the nodal-junction model of Hu and co-workers is largely unaffected by our band-structure arguments given above, thus complementing the overall *d*-wave 2D van Hove scenario for quasiparticle tunneling.

It is important to note that the spectral simulations would be characteristically different if an isotropic *s*-wave pairing symmetry were assumed. In such an *s*-wave 2D van Hove scenario, the absence of gap distribution would raise and sharpen the conductance peaks for the *c*-axis junction case while flattening the subgap conductance for both the *c*-axis and *a*-axis junction cases. This would lead to a more ''U-shaped'' spectral behavior, although the quasilinear background coming from the *a*-axis contribution would not change significantly, as could be seen by comparing Fig. 5 with the *s*-wave simulations given in Ref. 73. Furthermore, the ZBCP associated with a ''nodal'' junction in the *d*-wave scenario would not appear at all in such a non-nodal *s*-wave scenario,[51,52] regardless of the band structure.

It should also be noted that if the pairing symmetry were a mixture of *d* wave and *s* wave, the problem would involve a spectral superposition of the component symmetries depending on their relative amplitude and phase. In the $d+is$ scenario with *s* as the minor component, for example, one would expect the *c*-axis and *a*-axis junction cases to show additional subgap structures associated with the smaller *s*-wave gap.[54] For the nodal-junction case, a ZBCP structure could still occur as long as there is a phase sign change in the order parameter,[51,52] although the ZBCP would be split by broken time reversal symmetry.[50,53] These issues deserve more detailed investigation.[54] Here we merely observe that the absence of such mixed-symmetry spectral features in our tunneling data are consistent with a predominantly *d*-wave order parameter in the Hg-cuprates at 4.2 K, although the existence of a subdominant *s*-wave component at lower temperatures or in a magnetic field cannot be ruled out.[50,53]

VI. DATA INTERPRETATION AND DISCUSSION

These simulations illustrate the large variety of spectral behavior in the *d*-wave 2D van Hove scenario, sensitive to junction orientation, thickness and even the FS shape. This explains the remarkable diversity of tunneling results observed in the high-T_c cuprates. Spectral suppression associated with *a*-axis tunneling offers a natural band-structure explanation for the characteristic quasilinear background, without the need to invoke spurious effects or esoteric mechanisms. Spectral enhancement associated with tunneling *perpendicularly into* the *ab* plane provides a critical link between the enhanced-peak data and the *d*-wave 2D van Hove scenario by allowing a full manifestation of the quasiparticle DOS. Considering the spectral complexity introduced by the gap anisotropy and the band structure, any simple agreement with the BCS DOS would be fortuitous. And without precise control of the junction, no detailed comparison between data and model would be possible, particularly in the case of polycrystalline samples. For our data, the *d*-wave van Hove model does provide a general framework for spectral interpretation, with the simulations reproducing most of the generic spectral features.

Qualitatively speaking, each of the measured spectra shown in Fig. 1 can be described as a superposition of the thin-junction *c*-axis model [Fig. 6(a)] and the thick-junction *a*-axis model [Fig. 5(b)]. An equally weighted superposition of this sort is given in Fig. 7(a), demonstrating the resemblance to our data, particularly for Hg-1223 [Fig. 1(c)]. Such a ''combined'' junction could arise, for example, with the STM tip being in contact with a step edge between crystal platelets which are known to be abundant in cuprate samples. It could also happen if the tip were to break through a pristine *c*-axis crystal face, allowing *a*-axis tunneling to contribute. The latter scenario would explain why quasilinear spectral backgrounds are seen on our *c*-axis Hg-1212 films [Fig. 1(b)], especially when there is tip-sample contact. Essentially the *c*-axis contribution provides the enhanced gap peaks, while the *a*-axis contribution provides the quasi linear background. Peak width and subgap smearing could be adjusted through the barrier and broadening parameters d, U_0, k_BT, and Γ, while the spectral asymmetry and background slope could vary according to the specific band-structure parameters t, t', and μ. The degree of the asymmetry, for example, would increase with increasing t'. The sense of the asymmetry, on the other hand, would change with the doping level depending on where the vHs lies relative to the Fermi level μ. This latter possibility is demonstrated by another simulation of the ''combined'' junction, shown in Fig. 7(b), with the vHs shifted 10 meV below the Fermi level. Note that the shift has reversed the spectral asymmetry without altering the overall spectral features.

The overall band structure picture is supported by recent ARPES measurements on $YBa_2Cu_3O_{7+\delta}$ (YBCO) and

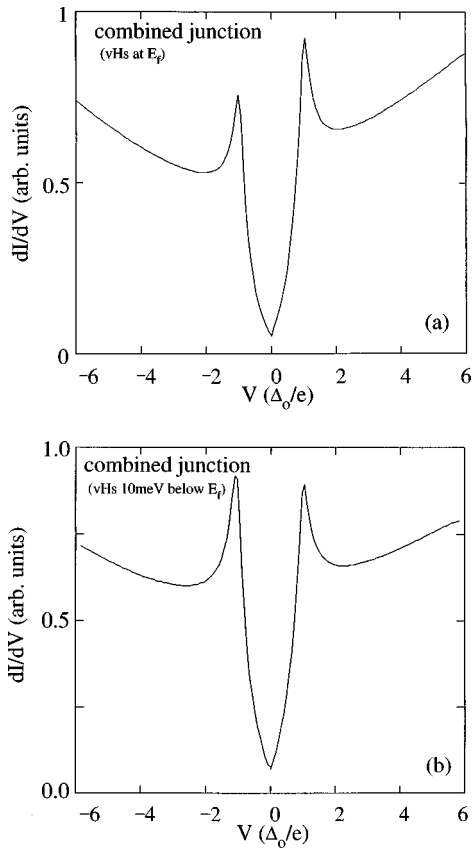

FIG. 7. Simulations of quasiparticle tunneling for a ''combined'' junction in the *d*-wave 2D van Hove scenario, using an equally weighted superposition of the thick *a*-axis [Fig. 5(b)] and thin *c*-axis junction [Fig. 6(a)]: (a) with the vHs directly at the Fermi level; (b) with the vHs shifted 10 meV below the Fermi level. Note that the doping level shift reverses the spectral asymmetry without altering the overall spectral features.

BSCCO, which show a characteristically denested Fermi surface that does *nearly* (within $\sim$20 meV) but not *directly* cross van Hove saddle points in the band structure.[19–21] In fact, these saddle points appear to be *extended* in the bottom half of the energy band, the vHs being more singular and asymmetric than described by the 2D tight-binding dispersion.[75,76] For our model, this *extended-vHs* scenario would imply: (1) stronger gap peaks for *c*-axis tunneling, because of the vHs enhancement; (2) steeper peak suppression and quasilinear background for *a*-axis tunneling, by virtue of the WKB breakdown; (3) larger spectral asymmetry, because of the increased band asymmetry about the Fermi level. These corrections could further improve agreement between our data and model, assuming that the Hg cuprates have similarly extended van Hove singularities.

We complete the data interpretation by addressing a noticeable midgap discrepancy between our data and model. It is apparent by inspection that the gap bottom is more rounded in the data than in the model, even if a larger broadening parameter were used. This problem is quite distinct in the Hg-1212 data [Fig. 1(b)], although pretty negligible for Hg-1223 [Fig. 1(c)]. It was also apparent in our fit of the Hg-1201 data to the vHs-enhanced *d*-wave DOS [Fig. 1(a)]. A plausible reason for the discrepancy could be the effects of impurity scattering on the nodal *d*-wave order parameter. Near a nodal line in the Brillouin zone, states with equal but opposite order parameter values are effectively averaged together by the impurity scattering.[77–79] This widens the gap nodes and increases the available states near midgap. The former implies a smaller distribution of gap values and therefore a more rounded low-bias spectral behavior. The latter leads naturally to zero-bias conductance, obviating the need for any smearing parameters to introduce states into the gap. Both effects would help to explain the midgap discrepancy between our data and model.

The overall consistency between our tunneling data and the *d*-wave 2D vHs model enables us to determine the *d*-wave gap maxima Δ_0 for the Hg cuprates. It is clear from our *c*-axis junction simulation in Fig. 6(a) that the gap peaks coincide with $\pm\Delta_0$ to fairly high accuracy. The vHs-enhanced *d*-wave gap singularities are relatively impervious to displacement by energy smearing because of their symmetric shape. Even if larger smearing parameters (lifetime, thermal, or otherwise) were introduced, these *d*-wave broadened singularities would not shift appreciably outward from $\pm\Delta_0$. This is in contrast to the asymmetrically shaped *s*-wave singularities which have the asymptotic square-root form. With little uncertainty, therefore, the *d*-wave energy-gap maxima can be taken as $\Delta_0 \approx 33$, 50, and 75 meV, respectively, for Hg-1201, Hg-1212, and Hg-1223, using the vHs-enhanced *d*-wave DOS fit presented earlier [Fig. 4(b)] as a heuristic example. These values correspond to reduced-gap ratios of $2\Delta_0/k_BT_C \approx 7.9$, 9.5, and 13, assuming optimally doped T_c values of 97, 123, and 135 K, respectively. These $2\Delta_0/k_BT_C$ ratios are substantially larger than the standard BCS value of 3.54,[86] but comparable to the large gap values reported for YBCO and BSCCO. For example, recent ARPES measurements on BSCCO indicate a *d*-wave energy gap with $\Delta_0 \approx 30$ meV $(2\Delta_0/k_BT_C \approx 8)$,[80] and $\Delta_0 \approx 27$ meV $(2\Delta_0/k_BT_C \approx 7.2)$.[81] Break-junction tunneling measurements on BSCCO and YBCO[82,83] indicate gap values of $\Delta_0 \approx 32$ meV $(2\Delta_0/k_BT_C \approx 8.6)$ and $\Delta_0 \approx 29$ meV $(2\Delta_0/k_BT_C \approx 7.6)$, respectively.

The reduced-gap values for the Hg cuprates can be compared with data for other high-T_c materials. A masterplot of $2\Delta_0/k_BT_C$ vs T_c is shown in Fig. 8. All the materials represented are presumed to have optimally doped T_c's. The STM tunneling data for the Hg cuprates reported in this work are indicated by solid circles and underlined labels. STM tunneling data from previous works[42,47] are indicated by open circles. The break-junction tunneling data on BSCCO, YBCO, its 60 K phase (YBCO-60 K) and $La_{2-x}Sr_xCuO_{4-x}$ (LSCO) are indicated by solid squares.[82–84] The point-contact junction data from $Nd_{2-x}Ce_xCuO_{4-y}$ NCCO, the noncuprate $Ba_{1-x}K_xBiO_3$ (BKBO) and Hg-1201 are indicated by solid triangles.[85,41] The ARPES data for BSCCO are indicated by asterisks.[80,81] Although a subset of all the published data, these data points are the most meaningful because they were taken from a selection of spectra which show distinct gap features. The break-junction tunneling and ARPES data are especially reliable since these measurements involve breaking the sample *in situ*, thus ensuring bulk stoichiometry. Considered together, these data suggest that for optimal doping $2\Delta_0/k_BT_C$ tends to increase with increasing T_c. The lower T_c materials hover just above the BCS weak-coupling limit of 3.54 and well within the conventional

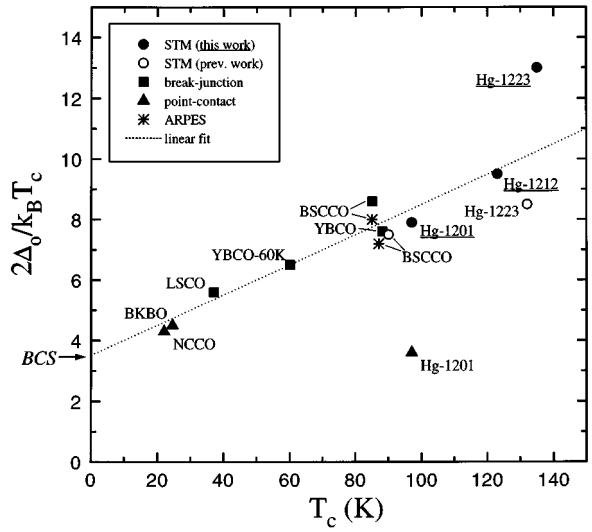

FIG. 8. Masterplot of $2\Delta_0/k_BT_c$ vs T_c for various high-T_c cuprates, including the noncuprate BKBO for comparison. All the materials represented are presumed to have optimally doped T_c's The STM tunneling data for the Hg cuprates reported in this work are indicated by solid circles and underlined labels. STM tunneling data from previous works (Refs. 42 and 47) are indicated by open circles. The break-junction tunneling data on BSCCO, YBCO, YBCO-60 K and LSCO are indicated by solid squares (Refs. 82–84). The point-contact junction data from NCCO, BKBO, and Hg-1201 are indicated by solid triangles (Refs. 41 and 85). The ARPES data for BSCCO are indicated by asterisks (Refs. 80 and 81). The plot reveals a dramatic deviation of $2\Delta_0/k_BT_c$ from BCS universality as T_c increases, as illustrated by the simple linear fit (dotted curve) through the BCS weak-coupling limit of 3.54.

strong-coupling regime ($\sim 3.6-5.2$).[86,87] The preponderance of data points at $2\Delta_0/k_BT_C \approx 6.5-8.5$ for the higher-T_c YBCO and BSCCO already indicates a serious deviation from the BSC range. The Hg-cuprate data suggest that $2\Delta_0/k_BT_C$ continues, to increase with elevated T_c. A simple linear fit is shown as the dotted curve in the masterplot to illustrate this upward trend, with the requirement that it approaches the BCS limit as $T_c \rightarrow 0$. In essence, whatever mechanism is responsible for enhancing the critical temperature seems also to be responsible for the deviation of the reduced-gap ratio from BCS universality. This correlation provides an important criterion for the understanding of high- T_c superconductivity.

VII. SUMMARY

In summary, we have presented quasiparticle tunneling spectra on the high-T_c superconductors $Hg_1Ba_2Ca_{n-1}Cu_nO_{2n+2+\delta}$ ($n=1,2,3$), and shown the spectra to be consistent with $d_{x^2-y^2}$ order parameter symmetry in the 2D van Hove scenario. The band structure appears to play a significant role in the tunneling: the 2D van Hove singularity enhances the quasiparticle density-of-states peaks, in conjunction with broadening by the nodal d-wave gap anisotropy; the low c-axis dispersion allows the spectral enhancement to be manifested, by effectively flattening out the tunneling cone; the saddle points in the energy dispersion along the a axis introduce severe wave vector mismatch across the tunnel junction, resulting in a quasilinear spectral slope through breakdown of the WKB approximation; the next-nearest-neighbor interaction in the CuO_2 lattice and doping dependence of the denested Fermi surface produce spectral asymmetry. The symmetric shape of the vHs-enhanced d-wave gap singularity makes it impervious to displacement by energy smearing, thus allowing accurate determination of the d-wave energy-gap maximum Δ_0. The reduced-gap ratios $2\Delta_0/k_BT_c$ were determined to be 7.9, 9.5, and 13, respectively, for optimally doped Hg-1201, Hg-1212, and Hg-1223. These values are substantially larger than the BCS weak coupling limit of 3.54. A comparison with data from other high-T_c cuprates indicates an overall trend of $2\Delta_0/k_BT_c$ rising with T_c, in violation of BCS universality. This trend suggests the large $2\Delta_0/k_BT_c$ to be intimately related to the T_c enhancement mechanism, providing another key criterion for the understanding of high-T_c superconductivity, along with the 2D van Hove scenario and d-wave order parameter symmetry.

ACKNOWLEDGMENTS

J.Y.T.W. would like to thank T. Jung, A. Levy, and J. Rosen for their valuable technical guidance, as well as D. M. Newns and M. Takigawa for helpful discussions. J.Y.T.W. is grateful to IBM T. J. Watson Research Center for hosting him (during his research), as well as to the University of Nijmegen for their hospitality during his visit. Critical reading of the manuscript by N.-C. Yeh was greatly appreciated. This work was supported by the Republic of China National Science Council, the New York State Institute on Superconductivity, and the State of Texas through the Texas Center for Superconductivity at the University of Houston.

*Present address: Dept. of Physics, California Institute of Technology, Pasadena, CA 91125.

†Present address: Dept. of Physics, University of Arkansas, Fayettville, AR 72701.

[1] E. L. Wolf, *Principles of Electron Tunneling Spectroscopy* (Oxford University Press, Oxford, 1985); C. B. Duke, *Tunneling in Solids* (Academic, New York, 1969).

[2] G. Bednorz and K. A. Muller, Z. Phys. B **64**, 189 (1986).

[3] M. K. Wu, J. R. Ashburn, C. J. Torng, R. L. Meng, L. Gao, Z. J. Huang, Y. Q. Wang, and C. W. Chu, Phys. Rev. Lett. **58**, 908 (1987).

[4] J. R. Kirtley, Int. J. Mod. Phys. B **4**, 201 (1990).

[5] T. Hasegawa, H. Ikuta, and K. Kitazawa, in *Physical Properties of High Temperature Superconductors III*, edited by D. M. Ginsberg (World Scientific, Singapore, 1992), p. 525.

[6] P. J. M. van Bentum and H. van Kempen, in *Scanning Tunneling Microscopy I*, edited by H. J. Guntherodt and R. Wiesendanger, Vol. 20 of *Springer Series in Surface Science* (Springer, Berlin, 1992), p. 201.

[7] J. R. Kirtley, Phys. Rev. B **41**, 7201 (1990).

[8] P. J. M. van Bentum *et al.*, Phys. Rev. Lett. **60**, 369 (1988).

[9] M. Tachiki, S. Steglich, F. Adrian, and H. Adrien, Z. Phys. B **80**, 161 (1990).

[10] W. A. Atkinson and J. P. Carbotte, Phys. Rev. B **51**, 1161 (1995).

[11] P. Monthoux, A. V. Balatsky, and D. Pines, Phys. Rev. B **46**, 14 803 (1992).

[12] N. Bulut and D. J. Scalapino, Phys. Rev. B **45**, 2371 (1992).
[13] P. W. Anderson and Z. Zou, Phys. Rev. Lett. **60**, 132 (1988); P. W. Anderson, *ibid.* **67**, 660 (1991).
[14] H. J. Tao, A. Chang, Farun Lu, and E. L. Wolf, Phys. Rev. B **45**, 10 622 (1992).
[15] C. M. Varma *et al.*, Phys. Rev. Lett. **63**, 1996 (1989).
[16] J. Hartge *et al.*, J. Phys. Chem. Solids **54**, 1359 (1993).
[17] C. C. Tsuei *et al.*, Phys. Rev. Lett. **73**, 593 (1994); J. R. Kirtley *et al.*, Europhys. Lett. **36**, 707 (1996); C. C. Tsuei *et al.*, Science **271**, 329 (1996); C. C. Tsuei *et al.* (unpublished).
[18] For examples, see D. Pines and P. Monthoux, J. Phys. Chem. Solids **56**, 1651 (1995); N. Bulut and D. J. Scalapino, Phys. Rev. B **54**, 14 971 (1996).
[19] Z. X. Shen *et al.*, Phys. Rev. Lett. **70**, 1553 (1993).
[20] D. S. Dessau *et al.*, Phys. Rev. Lett. **71**, 2781 (1993).
[21] R. Liu *et al.*, Phys. Rev. B **52**, 553 (1995).
[22] R. S. Markiewicz, J. Phys. Chem. Solids **54**, 1153 (1993); R. S. Markiewicz (unpublished).
[23] W. M. Que and G. Kirczenow, Phys. Rev. B **38**, 4601 (1988).
[24] T. Schneider, H. Deraedt, and M. Frick, Z. Phys. B **76**, 3 (1989).
[25] C. Zhou and H. J. Schulz, Phys. Rev. B **45**, 7397 (1992).
[26] F. Wenger and S. Ostlund, Phys. Rev. B **47**, 5977 (1993).
[27] K. Kouznetsov and L. Coffey, Phys. Rev. B **54**, 3617 (1996).
[28] J. Bok and J. Bouvier, Physica C **274**, 1 (1997).
[29] S. Gasiorowicz, *Quantum Physics* (Wiley, New York, 1974), pp. 84–86, Appendix 3.
[30] W. A. Harrison, Phys. Rev. **123**, 85 (1961).
[31] S. N. Putlin, E. V. Antipov, O. Chmaissem, and M. Marezio, Nature (London) **362**, 226 (1993).
[32] A. Schilling, M. Cantoni, J. D. Guo, and H. R. Ott, Nature (London) **363**, 56 (1993).
[33] C. W. Chu, L. Gao, F. Chen, Z. J. Huang, R. L. Meng, and Y. Y. Xue, Nature (London) **365**, 323 (1993); R. L. Meng *et al.*, Physica C **216**, 21 (1993).
[34] D. L. Novikov and A. J. Freeman, Physica C **212**, 233 (1993); C. O. Rodriguez, N. E. Christensen, and E. L. P. Blanca, *ibid.* **216**, 12 (1993).
[35] J. M. Harris, H. Wu, N. P. Ong, R. L. Meng, and C. W. Chu, Phys. Rev. B **50**, 3246 (1994); A. Carrington *et al.*, Physica C **234**, xx (1994).
[36] Q. Xiong *et al.*, Phys. Rev. B **50**, 10 346 (1994); M. Nunez-Regueiro *et al.*, Science **262**, 97 (1993); C. W. Chu *et al.*, Nature (London) **365**, 323 (1993).
[37] D. M. Newns *et al.*, Phys. Rev. Lett. **73**, 1695 (1994); C. C. Tsuei *et al.*, Chin. J. Phys. **31**, 795 (1993).
[38] F. Chen, Z. J. Huang, R. L. Meng, Y. Y. Sun, and C. W. Chu, Phys. Rev. B **48**, 16 047 (1993).
[39] Y. Kubo, Phys. Rev. B **50**, 3181 (1994).
[40] A. Carrington, A. P. Mackenzie, C. T. Lin, and J. R. Cooper, Phys. Rev. Lett. **69**, 2855 (1992).
[41] J. Chen, J. F. Zasadzinski, K. E. Grey, J. L. Wagner, and D. G. Hinks, Phys. Rev. B **49**, 3683 (1994).
[42] G. T. Jeong, J. I. Kye, S. H. Chun, S. Lee, S. I. Lee, and Z. G. Khim, Phys. Rev. B **49**, 15 416 (1994).
[43] C. Rossel, P. Bauer, J. Karpinski, A. Schilling, and A. Morawski (unpublished).
[44] C. C. Tsuei, A. Gupta, G. Trafas, and D. Mitzi, Science **263**, 1259 (1994).
[45] J. Y. T. Wei, Ph.D. thesis, Columbia University, New York, 1996.
[46] G. E. Blonder, M. Tinkham, and T. M. Klapwijk, Phys. Rev. B **25**, 4515 (1982).
[47] C. Renner and Ø. Fisher, Phys. Rev. B **51**, 9208 (1995); Physica C **235**, 53 (1994); B. Barbiellini, Ø Fischer, M. Peter, C. Renner, and M. Weger, *ibid.* **220**, 55 (1994).
[48] E. G. J. Boon, A. J. A. van Roy, and H. van Kempen, Physica C **235–240**, 1879 (1994); E. G. J. Boon and H. van Kempen (unpublished).
[49] D. Coffey and L. Coffey, Phys. Rev. Lett. **70**, 1529 (1993); Phys. Rev. B **53**, 15 292 (1996).
[50] For example, see, M. Covington *et al.*, Phys. Rev. Lett. **79**, 277 (1997), and references therein.
[51] C. R. Hu, Phys. Rev. Lett. **72**, 1526 (1994); (unpublished); J. Yang and C. R. Hu, Phys. Rev. B **50**, 16 766 (1994); J. H. Xu, J. H. Miller, and C. S. Ting, *ibid.* **53**, 3604 (1996).
[52] Y. Tanaka and S. Kashiwaya, Phys. Rev. Lett. **74**, 3451 (1995); S. Kashiwaya *et al.*, Phys. Rev. B **51**, 1350 (1995).
[53] M. Fogelstrom, D. Rainer, and J. A. Sauls, Phys. Rev. Lett. **79**, 281 (1997).
[54] J. Y. T. Wei, N.-C. Yeh, D. F. Garrigus, and M. Strasik (unpublished).
[55] D. V. Averin and K. K. Likharev, J. Low Temp. Phys. **62**, 345 (1986).
[56] H. R. Zeller and I. Giaever, Phys. Rev. **181**, 789 (1969).
[57] B. G. Orr, J. R. Clem, H. M. Jaeger, and A. M. Goldman, Phys. Rev. B **34**, 3491 (1987).
[58] I. Giaever, Phys. Rev. Lett. **5**, 147 (1960).
[59] R. C. Dynes, V. Narayanamurti, and J. P. Garno, Phys. Rev. Lett. **41**, 1509 (1978).
[60] H. Won and K. Maki, Phys. Rev. B **49**, 1397 (1994).
[61] J. Bardeen, Phys. Rev. Lett. **6**, 57 (1961).
[62] R. Stratton, J. Phys. Chem. Solids **23**, 1177 (1962).
[63] P. G. de Gennes, *Superconductivity of Metals and Alloys* (Benjamin, New York, 1966).
[64] G. D. Mahan, *Many Particle Physics* (Plenum, New York, 1990), Chap. 9.
[65] J. R. Schrieffer, *Theory of Superconductivity* (Benjamin, New York, 1964).
[66] G. Beuermann, Z. Phys. B **44**, 29 (1981).
[67] E. L. Wolf and G. B. Arnold, Phys. Rep. **91**, 31 (1982).
[68] M. H. Cohen, L. M. Falicov and J. C. Philips, Phys. Rev. Lett. **8**, 316 (1962).
[69] D. J. Ben Daniel and C. B. Duke, Phys. Rev. **160**, 679 (1967).
[70] D. C. Tsui, Phys. Rev. Lett. **24**, 303 (1970).
[71] J. V. Morgan and E. O. Kane, Phys. Rev. Lett. **3**, 466 (1959).
[72] R. T. Shuey, Phys. Rev. **137**, A1268 (1965).
[73] P. J. M. van Bentum and C. C. Tsuei, in *Superconductivity and Its Applications*,edited by H-S. Kwok *et al.*, AIP Conf. Proc. No. 273 (AIP, New York, 1992), p. 277.
[74] W. A. Harrison, *Solid State Theory* (Dover, New York, 1979); S. Datta, *Quantum Phenomena* (Addison-Wesley, Reading, MA, 1989).
[75] K. Gofron *et al.*, Phys. Rev. Lett. **73**, 3302 (1994).
[76] R. J. Kelly, J. Ma, C. Quitmann, G. Margaritondo, and M. Onellion, Phys. Rev. B **50**, 590 (1994).
[77] Hirschfeld-PJ, J. Phys. Chem. Solids **56**, 1605 (1995); K. Ziegler, M. H. Hettler, and P. J. Hirschfeld, Phys. Rev. Lett. **77**, 3013 (1996).
[78] R. Fehrenbacher and M. R. Norman, Phys. Rev. B **50**, 3495 (1994).
[79] T. Hotta, J. Phys. Soc. Jpn. **62**, 274 (1993).

[80] M. R. Norman, M. Randeria, H. Ding, and J. C. Campuzano, Phys. Rev. B **52**, 615 (1995).
[81] H. Ding *et al.*, Phys. Rev. Lett. **74**, 2784 (1995).
[82] Y. G. Ponomarev *et al.*, Phys. Rev. B **52**, 1352 (1995); Y. G. Ponomarev *et al.*, Physica C **243**, 167 (1995).
[83] D. Mandrus, J. Hartge, C. Kendziora, L. Mihaly, and L. Forro, Europhys. Lett. **22**, 199 (1993).
[84] H. Murakami, S. Ohbuchi, and R. Aoki, J. Phys. Soc. Jpn. **63**, 2653 (1994).
[85] J. F. Huang *et al.*, Nature (London) **347**, 369 (1990).
[86] J. Bardeen, L. N. Cooper, and J. R. Schrieffer, Phys. Rev. **108**, 1175 (1957).
[87] J. P. Carbotte, Rev. Mod. Phys. **62**, 1027 (1990).